

Article

# Visualization and Localization of Submicron-Sized Ammonium Sulfate Particles on Needles of Japanese Larch (*Larix kaempferi*) and Japanese Cedar (*Cryptomeria japonica*) and Leaves of Japanese Beech (*Fagus crenata*) and Japanese Chinquapin (*Castanopsis sieboldii*) after Artificial Exposure

Kenichi Yamane <sup>1,2</sup>, Satoshi Nakaba <sup>3</sup>, Masahiro Yamaguchi <sup>1,4</sup> , Katsushi Kuroda <sup>2</sup>, Yuzou Sano <sup>5</sup>, I. Wuled Lenggoro <sup>6</sup>, Takeshi Izuta <sup>3</sup> and Ryo Funada <sup>3,\*</sup>

<sup>1</sup> Faculty of Agriculture, Tokyo University of Agriculture and Technology, Fuchu, Tokyo 183-8509, Japan; coxken24@gmail.com (K.Y.); masah-ya@nagasaki-u.ac.jp (M.Y.)

<sup>2</sup> Forestry and Forest Products Research Institute, 1 Matsunosato, Tsukuba, Ibaraki 305-8687, Japan; kurodak@affrc.go.jp

<sup>3</sup> Institute of Agriculture, Tokyo University of Agriculture and Technology, Fuchu, Tokyo 183-8509, Japan; nakaba@cc.tuat.ac.jp (S.N.); izuta@cc.tuat.ac.jp (T.I.)

<sup>4</sup> Graduate School of Fisheries and Environmental Sciences, Nagasaki University, Nagasaki 852-8521, Japan

<sup>5</sup> Research Faculty of Agriculture, Hokkaido University, Sapporo, Hokkaido 060-8589, Japan; pirika@for.agr.hokudai.ac.jp

<sup>6</sup> Institute of Engineering, Tokyo University of Agriculture and Technology, Koganei, Tokyo 184-8588, Japan; wuled@cc.tuat.ac.jp

\* Correspondence: funada@cc.tuat.ac.jp; Tel.: +81-42-367-5716

Received: 15 November 2019; Accepted: 14 December 2019; Published: 17 December 2019



**Abstract:** We applied a method combining field-emission scanning electron microscopy (FE-SEM) with energy dispersive X-ray spectrometry (EDX) to visualize the deposition and localization of the submicron-sized ammonium sulfate (AS) particles. The AS particles emitted from an aerosol generator in the laboratory were spherical in shape and individually deposited without aggregation on the surface of a silicon substrate. We determined the AS particles on the surfaces of the needles of Japanese larch (*Larix kaempferi*) and Japanese cedar (*Cryptomeria japonica*), and the leaves of Japanese beech (*Fagus crenata*) and Japanese chinquapin (*Castanopsis sieboldii*), using EDX. The particles were deposited on either the adaxial or abaxial side of the leaves and needles. The AS particles deposited on the surfaces of the leaves and needles did not aggregate, and they were deposited on the surfaces of the leaves and needles in the same manner, regardless of leaf structure. These results, using a new method, highlight the early stages of the deposition and localization of submicron-sized AS particles on the surfaces of the leaves and needles of forest trees.

**Keywords:** ammonium sulfate particles; submicron-sized particles; field-emission scanning electron microscopy (FE-SEM); energy dispersive X-ray spectrometry (EDX)

## 1. Introduction

Recent increases in energy consumption in Asia have led to a rapid escalation in the anthropogenic emissions of air pollutants and their precursors [1,2]. As the increase in anthropogenic emissions in Asia is expected to continue into the future [2–4], the effects of air pollutants on Asian forest

ecosystems are of great concern. Forests have important functions, such as protecting biodiversity, producing biomass, fixing carbon dioxide, conserving soil, and protecting watersheds. Aerosol particles deposited on plant leaf surfaces may affect the growth, physiology, and surface conditions of leaves [5]. Anthropogenic emissions mainly consist of submicron-sized particles [6]. In addition to the 1–5 µm diameter-sized particles that are present on the surfaces of leaves under natural conditions, submicron-sized particles are mainly detected on the leaf surface [7]. These particles consist of multiple elements under natural atmospheric conditions [8,9]. For understanding the deposition mechanism of these particles, it is important to clarify the mechanism of deposition and the uptake of submicron-sized particles containing one element from the leaf surface. However, only a few observations of these specialized submicron-sized particles on the surface of leaves and needles are available. Burkhardt et al. [10] reported the deposition of submicron-sized di-2-ethylhexyl-sebacate (DES) particles in the stomatal regions of conifer needles. Submicron-sized lead particles have been observed inside the stomatal openings of lettuce after exposure to atmospheric metal contamination [11]. Grantz et al. [12] reported the deposition of submicron-sized sodium fluorescein aerosol on the surface of a leaf of broad bean. Thus, it is important to analyze the deposition and localization of general anthropogenic submicron-sized particles on leaves to assess the effects of these particles on trees.

We previously conducted an exposure experiment on leaf and needle surfaces to submicron-sized black carbon (BC) particles to clarify the effects of BC particles on forest tree species [13–15]. We also developed a visualization method to determine the deposition and localization of submicron-sized BC particles on tree leaves and needles using field-emission scanning electron microscopy (FE-SEM) [13]. Our findings revealed that (1) carbon-based particles were aggregated on leaves, and (2) carbon-based particles were deposited on the sparse waxy structural area in *Cryptomeria japonica* [14]. The amount of accumulated BC on the surfaces of leaves and needles of evergreen tree species Japanese chinquapin (*Castanopsis sieboldii*) and Japanese cedar (*Cryptomeria japonica*) was higher than those on deciduous tree species Japanese beech (*Fagus crenata*) and Japanese larch (*Larix kaempferi*) [16]. However, no significant changes in physiological data, such as net photosynthetic rates, growth, leaf temperature, or plugging of stomata, were observed after the trees had been exposed to BC particles [16]. On the other hand, Coccozza et al. [17] indicated that the foliar application of Ag-nanoparticles decreased the growth, aboveground biomass, and stem length in poplar, but not in oak and pine. These differences of results among tree species may be caused by the variation of the surface structures of leaves and needles.

To investigate the effects of particles, including the chemical composition on forest trees, Yamaguchi et al. [15,18] clarified the effects of submicron-sized ammonium sulfate (AS) particles on the physiology of four Japanese forest tree species, such as *Larix kaempferi*, *Cryptomeria japonica*, *Fagus crenata*, and *Castanopsis sieboldii*. AS is the dominant fine particle chemical species in Japan [19] and China [9]. Thus, understanding the effect of submicron-sized AS particles on forest trees is important. However, Yamaguchi et al. [15,18] reported no significant changes in the growth or net photosynthetic rates of *Larix kaempferi*, *Fagus crenata*, or *Castanopsis sieboldii*, but the net photosynthetic rate of the current-year needles increased, and that of previous-year needles decreased in *Cryptomeria japonica* after long-term exposure to AS particles. The relationship between the physiological changes and the presence of AS particles on the surfaces of the leaves and needles remains unknown. Therefore, clarifying where AS particles are deposited on the surfaces of leaves and needles is necessary in order to understand the effect of submicron-sized AS particles on forest trees in greater detail.

In this study, we applied a method to visualize the deposition of submicron-sized AS particles on the surfaces of leaves and needles, and analyzed the localization of these particles, after experimental exposure, onto four general habit forest tree species in Japan.

## 2. Materials and Methods

### 2.1. Plant Materials

We used leaves from two-year-old *Fagus crenata*, *Castanopsis sieboldii*, and *Cryptomeria japonica* seedlings, as well as one-year-old *Larix kaempferi* seedlings growing in a chamber at the Tokyo University of Agriculture and Technology in Fuchu, Tokyo, Japan [18]. There were 60 seedlings per tree species in the chamber [18]. We collected three current leaves of *Fagus crenata*, *Castanopsis sieboldii*, *Cryptomeria japonica*, and *Larix kaempferi*, and three previous-year leaves of *Cryptomeria japonica* in 2012 and 2013.

### 2.2. Exposure to Ammonium Sulfate Particles

The AS solution (0.1% *w/v*) was prepared as described by Yamaguchi et al. [18]. Fresh leaves and silicon substrates (controls) were artificially exposed to dried AS particles generated by an aerosol generator, specifically, an ultrasonic nebulizer (NE-U17; Omron Healthcare Co. Ltd., Kyoto, Japan), using ultrasonic force. The starting solution and the sprayed droplets included a solute, which was then dried to submicron-sized solid particles. The mean particle diameter was about 300 nm [18]. The particles were dried in a tube filled with silica gel before exposure [20]. Either the adaxial or abaxial side of the leaves was exposed to the AS particles for 3–30 min so as to observe the submicron-sized particles. As the deliquescence relative humidity of AS is about 80% at room temperature [21], the relative humidity in the exposure chamber was maintained at <70% to avoid the deliquescence of the dried AS particles.

### 2.3. FE-SEM and Energy Dispersive X-ray Spectrometry (EDX) Analysis

After exposure to AS, the leaves and silicon substrates were collected, cut into 5 × 5 mm squares with a razor blade, and air-dried for three days in a desiccator under 50% relative humidity. The air-dried samples were coated with carbon using a vacuum evaporator (TB500; Quorum Technologies, Guelph, ON, Canada). The particles deposited on the leaves and silicon substrates were observed by FE-SEM (S-4800; Hitachi, Tokyo, Japan) at accelerating voltages of 3, 5 (for observation of surface of leaves and silicon substrates), or 10 kV for the distinction between the particles and waxy structures on the leaves and needles [14]. Then, the particles and leaves were analyzed using EDX (Genesis-XM2, EDAX Inc., Mahwah, NJ, USA) at an accelerating voltage of 10 kV [22], and a current emission of 20–30 μA and a spot size of 1.

## 3. Results and Discussion

### 3.1. Visualization of Deposited Ammonium Sulfate Particles on the Surfaces of Needles and Leaves after Exposure

Numerous spherical particles were deposited individually on the silicon substrate without aggregation after exposure to the AS particles at a 70% relative humidity (Figure 1a). The diameters of the individual particles measured from the FE-SEM images were 300–600 nm (Figure 1a). A point analysis of Spot 1 by EDX revealed clear peaks corresponding to silicon (Si) and S (Figure 1c). In contrast, the EDX spectrum of Spot 2 only showed a peak corresponding to Si (Figure 1d). Thus, we concluded that the 300–600 nm diameter spherically-shaped particles and the sulfur (S) were derived from the AS solution.

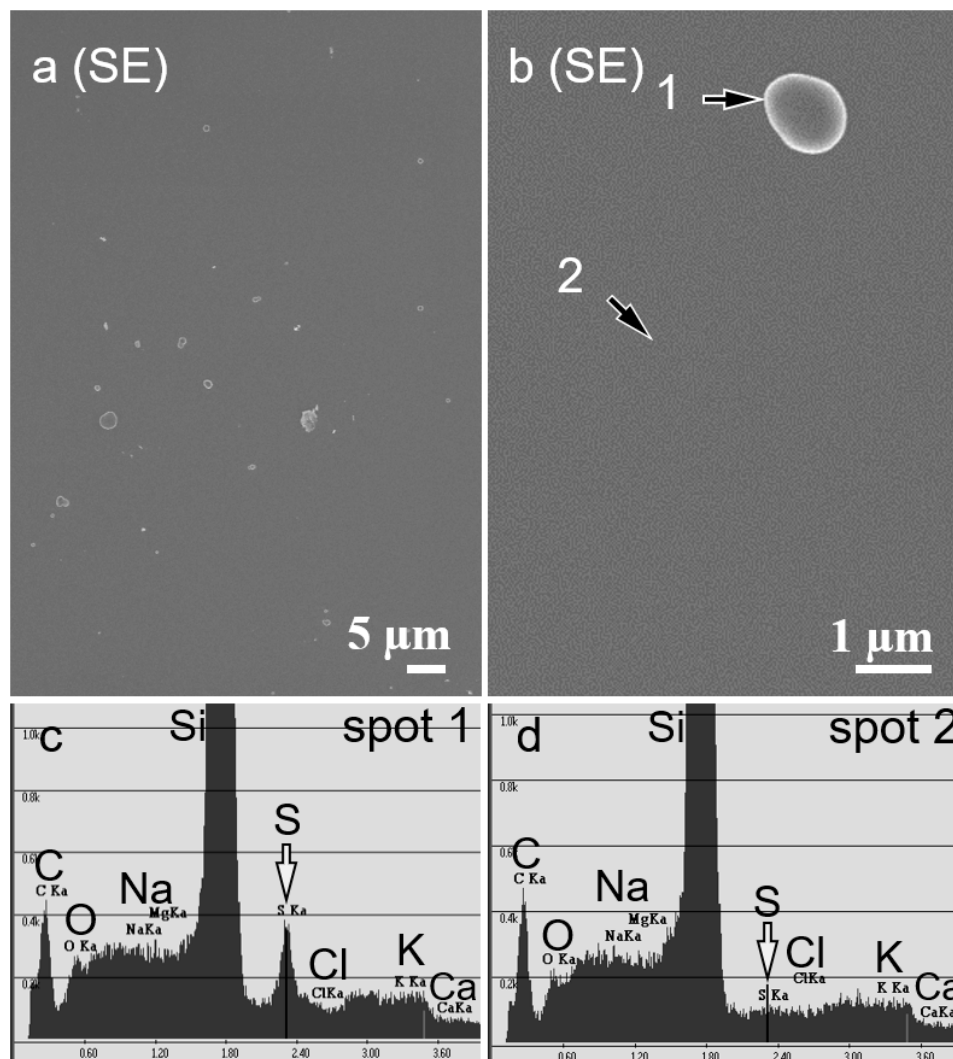


**Figure 1.** Secondary electron images captured by field-emission scanning electron microscope (FE-SEM) and energy dispersive X-ray spectrometry (EDX) spectra of the silicon substrates. (a) Ammonium sulfate (AS) particles (diameter 300–600 nm) were distributed on the silicon substrates and were not aggregated. (b) Higher magnification image of an AS particle. (c) EDX spectrum of Spot 1 in (b) showing a clear peak corresponding to sulfur. (d) EDX spectrum of Spot 2 in (b). No peaks corresponding to sulfur were obtained from the silicon substrate. Black arrows indicate focal points for the EDX analysis. White arrows indicate sulfur peaks.

Several types of waxy structures, such as threads, tubules, clusters of tubules, and plates, were observed on the surfaces of the leaves and needles [23]. Although the secondary electron images revealed a clear distinction between the waxy structures and particles on the smooth leaf surfaces at a high magnification, the secondary low magnification electron images failed to distinguish between the waxy structures and particles on the leaf surfaces covered with tubules (Figure 2a). Therefore, in addition to the secondary electron images, we obtained backscattered electron images at an accelerating voltage of 10 kV, so as to reflect the composition of the particles (Figure 2b). As the particles consisted of heavier elements, such as sulfur (S), than the wax composed of carbon (C), we could distinguish the AS particles from the waxy structures as white specks (Figure 2b).

We observed various sizes of particles on the leaves and needles after exposure to AS under 70% relative humidity (Figure 2a,b). The EDX spectrum revealed small peaks from the surfaces of the leaves and needles corresponding to S (Figure 2f). In contrast, clear S peaks were detected in other particles (Figure 2c–e).

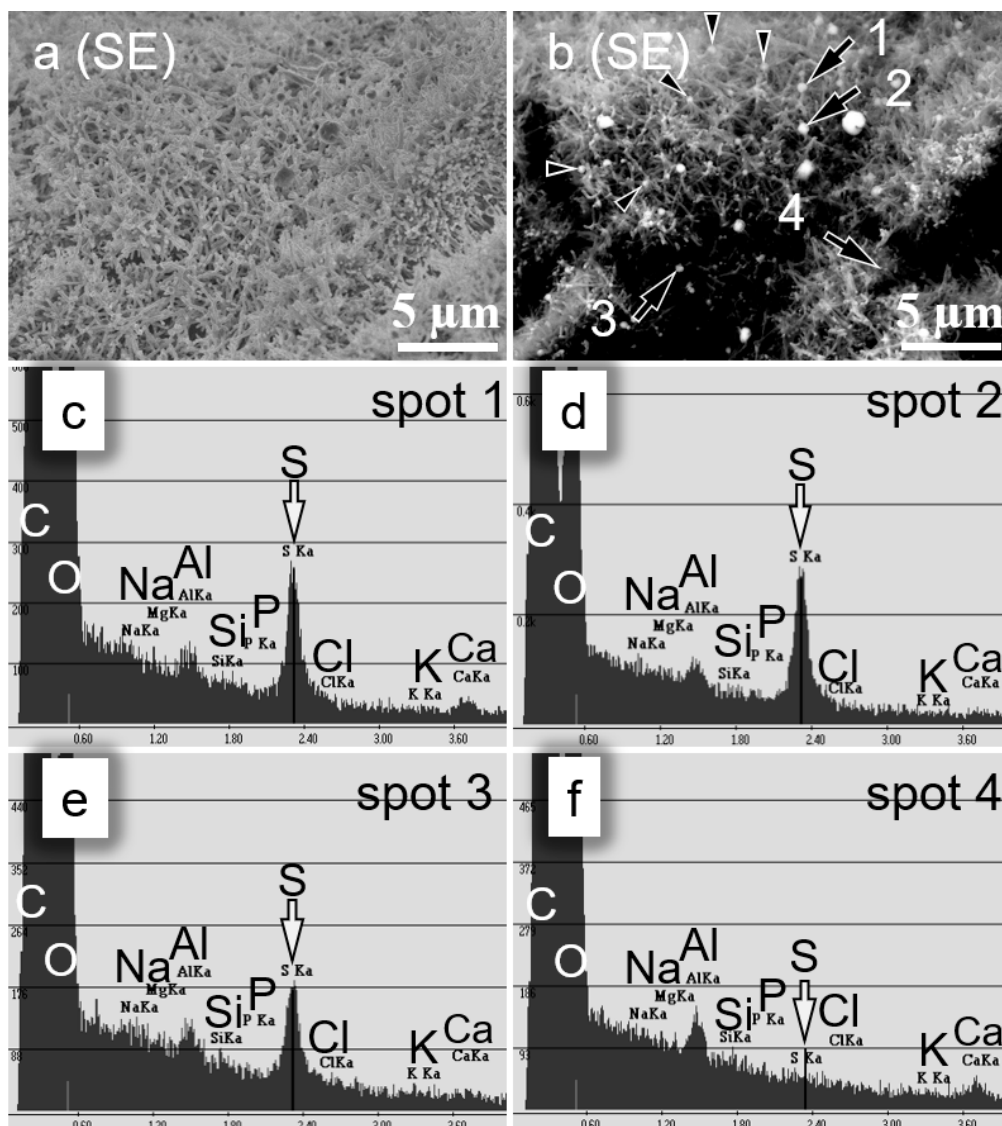


**Figure 2.** Secondary electron images captured by field-emission scanning electron microscope (FE-SEM) and energy dispersive X-ray spectrometry (EDX) spectra of leaves from Japanese cedar (*Cryptomeria japonica*) seedlings. (a) Secondary electron image of leaves from seedlings after exposure to ammonium sulfate (AS) particles. The leaf surface was covered with waxy structures. (b) Backscattered electron image of the leaves corresponding to (a). AS particles (white specks) contrasted with the waxy structures. (c–f). EDX spectra of spots 1 (c), 2 (d), 3 (e), and 4 (f) in (b). Clear peaks corresponding to sulfur were observed in particles (c–e), but no peak was observed in areas without such particles (f). Black arrows indicate focal points for the EDX analysis. Arrowheads indicate indistinguishable particles from the waxy structures shown in (a). White arrows indicate sulfur peaks.

EDX is an analytical method to identify elements according to the characteristic the X-rays generated when an object is irradiated with an electron beam. The X-rays are generated from the surface to several micrometers deep of the irradiated objects. Thus, these characteristic X-rays were generated from submicron-sized particles on the leaves and needles, and they deposited particles at a submicron scale. The leaves and needles of the woody plants generally include S under natural conditions [24,25]. Therefore, the characteristic X-rays from S derived from the leaves and needles must be distinguished from those derived from the deposited particles. The peak corresponding to S derived from the AS particles was sharp, whereas the signal intensity corresponding to S was negligible



on the leaf and needle surfaces with no particles (Figure 2f). Therefore, we concluded that the sharp S peak was derived from the AS particles.

We conducted spot and area analyses (elemental mapping) using EDX to determine the deposition of particles on the leaves and needles (Figure 3b). After obtaining a secondary electron image of the leaf surface (Figure 3a), we scanned the same area of the leaf surface for 60 min. The sharp peak corresponding to S derived from the area was detected in red (Figure 3b). The particles on the elemental mapping images were displayed in red (Figure 3b, arrowhead) or white (Figure 3b, white star), among similar shapes and sizes of particles. As the leaf was damaged due to the strong beam being applied for a long time, the shapes of the particles were different between Figure 3a and 3b. Although the EDX area analysis was useful for identifying whole particles on the leaves and needles, at least 60 min was required to scan a single area at 10,000 counts/s, and this analysis may have damaged the sample. These values depended on the sample condition, such as the surface microstructure and the charge of the sample. Thus, an area analysis was not suitable for determining whether particles including S were deposited on the surfaces of the leaves and needles. Therefore, we conducted a point analysis using EDX to confirm the localization of the AS particles in the subsequent experiments.

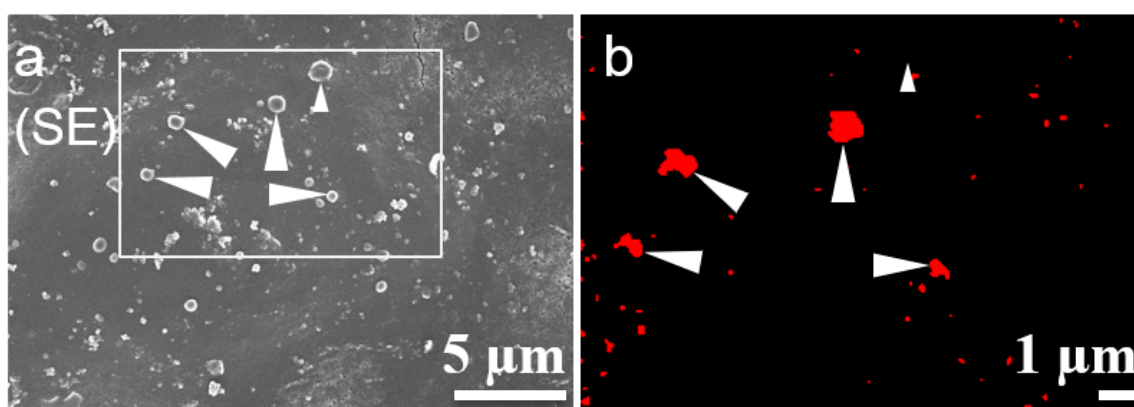


**Figure 3.** Field-emission electron scanning microscopy (FE-SEM) and energy dispersive X-ray spectrometry (EDX) images of ammonium sulfate (AS) particles on leaves from Japanese beech (*Fagus crenata*) seedlings. (a) Secondary electron image of leaves from *Fagus crenata* seedlings after exposure to AS particles. Non-aggregated AS particles were distributed on the leaves. (b) Elemental mapping image of the area marked by the rectangle in (a). Particles containing sulfur are shown in red. Arrowheads indicate particles containing sulfur. Small arrowhead indicates a particle without sulfur.

### 3.2. Localization of Ammonium Sulfate Particles on the Surface of Leaves and Needles

The AS particles were distributed individually and did not aggregate on the surfaces of the leaves or needles (Figure 4a–f), which was similar to the result for the silicon substrate (Figure 1). On FE-SEM, the relationship between vacuum-driven evaporation and the corresponding shrinkage (or movement) of AS particles on the leaf surface was difficult to determine. We observed no differences in the localization of the particles as a function of the exposure duration. When the relative humidity in the vicinity of the leaves and needles was high, changes in the shape and size of the AS particles deposited may have been attributed to deliquescence. In our experiments, we did not observe an effect of deliquescence during the 3–30 min exposure. A relatively large number of particles was deposited on the leaf surface facing the exposure, regardless of the side exposed (i.e., adaxial or abaxial side of leaves). Waxy structures were distributed irregularly on the surfaces of the conifer needles [26]. Although the needle surface was covered thickly with tube-like waxy structures at the periphery of the stomata, the needle surface was covered thinly with waxy structures distant from the stomata [23]. AS particles were deposited on both dense (Figure 4a,c) and sparse (Figure 4b,d) areas with waxy structures. The distribution of waxy structures was generally not uniform in the coniferous species [27,28]. The AS particles were also evenly deposited from the center to the edges of the leaves

and needles. Although the waxy structures on the current *Cryptomeria japonica* needles were more conspicuous than those on the previous-year needles, the AS particles were deposited in the same manner on both the current and previous-year needles. Although the leaf and needle microstructure of the four trees species used in this study were different, the AS particles were deposited in the same manner on the leaf and needle surfaces. In contrast, the BC particles were deposited as aggregates only on the sparse area of the waxy structures of the needles of *Cryptomeria japonica* [14]. An EDX analysis cannot detect individual BC particles on the leaf surface, because both consist of carbon. Therefore, the black carbon particles were identified by their shape and aggregation [14]. In contrast, in the present study, the AS particles were identified by FE-SEM/EDX analysis. These results indicate that the pattern of the deposition and aggregation of the AS particles clearly differed from those of the BC particles. The differences between the deposition patterns of the AS and BC particles might be attributed to the unique properties of each of substance, such as wettability and ionization capability.

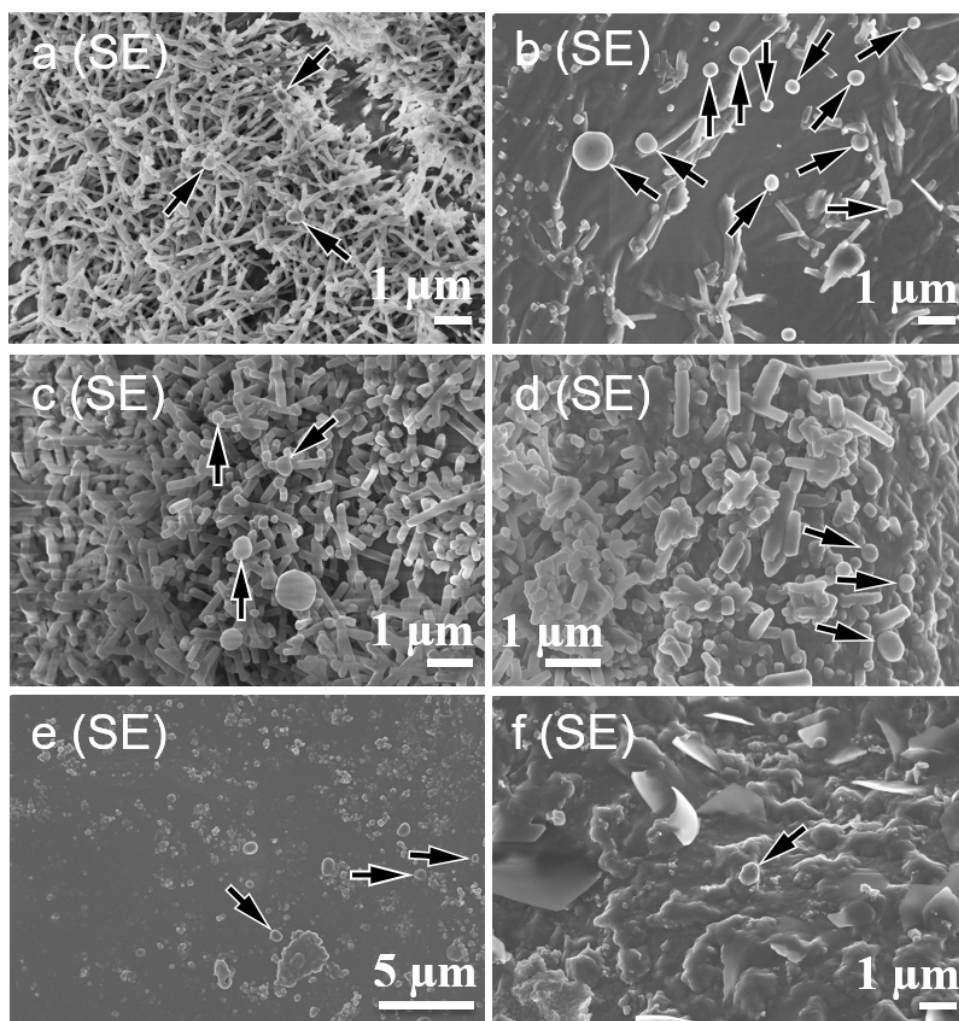


**Figure 4.** The secondary electron images of the leaves and needles after exposure to ammonium sulfate (AS) particles: *Cryptomeria japonica* (a,b), Japanese larch (*Larix kaempferi*) (c,d), *Fagus crenata* (e), and Japanese chinquapin (*Castanopsis sieboldii*) (f). The surfaces of the leaves were either covered with tubules (a,c), smooth layers (e), and plates (f) of waxy structures, or rarely covered with these structures (b,d). AS particles were deposited on both dense (a,c) and sparse (b,d) areas of the waxy tubule structures. Black arrows indicate AS particles.

#### 4. Conclusions

We applied a method to visualize the deposition of individual submicron-sized AS particles on leaf and needle surfaces by FE-SEM and EDX. This method provides us a detailed localization of the submicron-sized AS particles immediately after deposition. Our current and previous studies [14] revealed that the deposition patterns of AS particles on the surfaces of leaves and needles differed from those of the BC particles. The proposed method will be useful to determine the localization pattern of other submicron-sized particles, including elements that can be detected by EDX.

**Author Contributions:** conceptualization, T.I. and R.F.; methodology and investigation, K.Y., S.N., M.Y., K.K., Y.S., and I.W.L.; writing (original draft preparation), K.Y.; writing (review and editing), S.N., M.Y., K.K., Y.S., I.W.L., T.I., and R.F.

**Funding:** This study was supported by JSPS Grants-in-Aid for Scientific Research (KAKENHI), grant numbers 20120009 and 20120010.

**Acknowledgments:** The authors thank Masao GEN and Akito SEKI from the laboratory of Wuled Lenggoro, Graduate School of Bio-Applications and Systems Engineering, Tokyo University of Agriculture and Technology, for providing technical support regarding the ammonium sulfate particle exposure.

**Conflicts of Interest:** The authors declare no conflict of interest.

#### References

- Ohara, T.; Kurokawa, J. Long-term variation of air pollutants related to atmospheric aerosol in Asia, China and Japan. *Eaorozu Kenkyu* **2018**, *33*, 95–101. (In Japanese) [[CrossRef](#)]
- Ohara, T.; Akimoto, H.; Kurokawa, J.; Horii, N.; Yamaji, K.; Yan, X.; Hayasaka, T. An Asian emission inventory of anthropogenic emission sources for the period 1980–2020. *Atmos. Chem. Phys.* **2007**, *7*, 4419–4444. [[CrossRef](#)]
- Akimoto, H. Global Air Quality and Pollution. *Science* **2003**, *302*, 1716–1719. [[CrossRef](#)] [[PubMed](#)]
- Sun, W.; Shao, M.; Granier, C.; Liu, Y.; Ye, C.S.; Zheng, J.Y. Long-Term Trends of Anthropogenic SO<sub>2</sub>, NO<sub>x</sub>, CO, and NMVOCs Emissions in China. *Earth's Future* **2018**, *6*, 1112–1133. [[CrossRef](#)]
- Motai, A.; Yamazaki, M.; Muramatsu, N.; Watanabe, M.; Izuta, T. Submicron ammonium sulfate particles deposited on leaf surfaces of a leafy vegetable (*Komatsuna*, *Brassica rapa* L. var. *perviridis*) are taken up by leaf and enhance nocturnal leaf conductance. *Atmos. Environ.* **2018**, *187*, 155–162. [[CrossRef](#)]
- Horvath, H. Aerosols—An introduction. *J. Environ. Radioact.* **2000**, *51*, 5–25. [[CrossRef](#)]
- Neinhuis, C.; Barthlott, W. Seasonal changes of leaf surface contamination in beech, oak, and ginkgo in relation to leaf micromorphology and wettability. *New Phytol.* **1998**, *138*, 91–98. [[CrossRef](#)]
- Freney, E.J.; Adachi, K.; Buseck, P.R. Internally mixed atmospheric aerosol particles: Hygroscopic growth and light scattering. *J. Geophys. Res.* **2010**, *115*, D19210. [[CrossRef](#)]
- Fu, H.; Zhang, M.; Li, W.; Chen, J.; Wang, L.; Quan, X.; Wang, W. Morphology, composition and mixing state of individual carbonaceous aerosol in urban Shanghai. *Atmos. Chem. Phys.* **2012**, *12*, 693–707. [[CrossRef](#)]
- Burkhardt, J.; Peters, K.; Crossley, A. The presence of structural surface waxes on coniferous needles affects the pattern of dry deposition of fine particles. *J. Exp. Bot.* **1995**, *46*, 823–831. [[CrossRef](#)]
- Uzu, G.; Sobanska, S.; Sarret, G.; Muñoz, M.; Dumat, C. Foliar lead uptake by Lettuce exposed to atmospheric fallouts. *Environ. Sci. Technol.* **2010**, *44*, 1036–1042. [[CrossRef](#)] [[PubMed](#)]
- Grantz, D.A.; Zinsmeister, D.; Burkhardt, J. Ambient aerosol increases minimum leaf conductance and alters the aperture–flux relationship as stomata respond to vapor pressure deficit (VPD). *New Phytol.* **2018**, *219*, 275–286. [[CrossRef](#)] [[PubMed](#)]
- Yamane, K.; Nakaba, S.; Yamaguchi, M.; Kuroda, K.; Sano, Y.; Lenggoro, I.W.; Izuta, T.; Funada, R. Visualization of artificially deposited submicron-sized aerosol particles on the surfaces of leaves and needles in trees. *Asian J. Atmos. Environ.* **2012**, *6*, 275–280. [[CrossRef](#)]
- Nakaba, S.; Yamane, K.; Fukahori, M.; Nugroho, W.D.; Yamaguchi, M.; Kuroda, K.; Sano, Y.; Lenggoro, I.W.; Izuta, T.; Funada, R. Effect of epicuticular wax crystals on the localization of artificially deposited sub-micron carbon-based aerosols on needles of *Cryptomeria japonica*. *J. Plant Res.* **2016**, *129*, 873–881. [[CrossRef](#)]
- Yamaguchi, M.; Izuta, T. Effects of Black Carbon and Ammonium Sulfate Particles on Plants. In *Air Pollution Impacts on Plants in East Asia*; Izuta, T., Ed.; Springer: Tokyo, Japan, 2017; pp. 295–308. [[CrossRef](#)]



16. Yamaguchi, M.; Otani, Y.; Takeda, K.; Lenggoro, I.W.; Ishida, A.; Yazaki, K.; Noguchi, K.; Sase, H.; Murao, N.; Nakaba, S.; et al. Effects of long-term exposure to black carbon particles on growth and gas exchange rates of *Fagus crenata*, *Castanopsis sieboldii*, *Larix kaempferi* and *Cryptomeria japonica* seedlings. *Asian J. Atmos. Environ.* **2012**, *6*, 259–267. [[CrossRef](#)]
17. Cocozza, C.; Perone, A.; Giordano, C.; Salvatici, M.C.; Pignattelli, S.; Raio, A.; Schaub, M.; Sever, K.; Innes, J.L.; Tognetti, R.; et al. Silver nanoparticles enter the tree stem faster through leaves than through roots. *Tree Physiol.* **2019**, *39*, 1251–1261. [[CrossRef](#)]
18. Yamaguchi, M.; Otani, Y.; Li, P.; Nagao, H.; Lenggoro, I.W.; Ishida, A.; Yazaki, K.; Noguchi, K.; Nakaba, S.; Yamane, K.; et al. Effects of long-term exposure to ammonium sulfate particles on growth and gas exchange rates of *Fagus crenata*, *Castanopsis sieboldii*, *Larix kaempferi* and *Cryptomeria japonica* seedlings. *Atmos. Environ.* **2014**, *97*, 493–500. [[CrossRef](#)]
19. Takami, A.; Miyoshi, T.; Shimono, A.; Kaneyasu, N.; Kato, S.; Kajii, Y.; Hatakeyama, S. Transport of anthropogenic aerosols from Asia and subsequent chemical transformation. *J. Geophys. Res.* **2007**, *112*, D22S31. [[CrossRef](#)]
20. Hori, M.; Ohta, S.; Murao, N.; Yamagata, S. Activation capability of water soluble organic substances as CCN. *J. Aerosol Sci.* **2003**, *34*, 419–448. [[CrossRef](#)]
21. Brooks, S.D. Deliquescence behavior of organic/ammonium sulfate aerosol. *Geophys. Res. Lett.* **2002**, *29*, 23-1–23-4. [[CrossRef](#)]
22. Watanabe, Y.; Yamaguchi, T.; Katata, G.; Noguchi, I. Aerosol deposition and behavior on leaves in cool-temperate deciduous forests. Part 1: A preliminary study of the effect of fog deposition on behavior of particles deposited on the leaf surfaces by microscopic observation and leaf-washing technique. *Asian J. Atmos. Environ.* **2013**, *7*, 1–7. [[CrossRef](#)]
23. Barthlott, W.; Neinhuis, C.; Cutler, D.; Ditsch, F.; Meusel, I.; Theisen, I.; Wilhelm, H. Classification and terminology of plant epicuticular waxes. *Bot. J. Linn. Soc.* **1998**, *126*, 237–260. [[CrossRef](#)]
24. Legris-Delaporte, S.; Ferron, F.; Landry, J.; Costes, C. Metabolization of elemental sulfur in wheat leaves consecutive to its foliar application. *Plant Physiol.* **1987**, *85*, 1026–1030. [[CrossRef](#)] [[PubMed](#)]
25. Adams, W.W.; Winter, K.; Schreiber, U.; Schramel, P. Photosynthesis and chlorophyll fluorescence characteristics in relationship to changes in pigment and element composition of leaves of *Platanus occidentalis* L. during autumnal leaf senescence. *Plant Physiol.* **1990**, *92*, 1184–1190. [[CrossRef](#)] [[PubMed](#)]
26. Hanover, J.W.; Reicosky, D.A. Surface wax deposits on foliage of *Picea pungens* and other conifers. *Am. J. Bot.* **1971**, *58*, 681–687. [[CrossRef](#)]
27. Huttunen, S. Effects of Air Pollutants on Epicuticular Wax Structure. In *Proceedings of the Air Pollutants and the Leaf Cuticle*; Percy, K.E., Cape, J.N., Jagels, R., Simpson, C.J., Eds.; Springer: Berlin/Heidelberg, Germany, 1994; pp. 81–96. [[CrossRef](#)]
28. Grodzińska-Jurczak, M. Conifer epicuticular wax as a biomarker of air pollution: An overview. *Acta Soc. Bot. Pol.* **1998**, *67*, 291–300. [[CrossRef](#)]

